Original Article

Bulletin of Pure and Applied Sciences.
Vol.37 C (Chemistry), No.1, 2018: P.6-11
Print version ISSN 0970 4620
Online version ISSN 2320 320X
DOI 10.5958/2320-320X.2018.00002.X

Structural, Bonding and Spectral Analysis of an anti-malarial drug 5-(4-chloro phenyl)-6-ethyl-2,4-pyrimidinediamine

Y. Sheeba Sherlin[1], T.Vijayakumar[2], J.Binoy[3], S.D.D. Roy[4] and V.S. Jayakumar[5,*]

Author Affiliations
[1]Dept. of Physics, Scott Christian College (Autonomous), Nagercoil-629003, Tamil Nadu.
[2] Dept. of Physics & Nanotechnology, SRM University, Kattankulathur-603203, Tamil Nadu, India.
[3] Dept. of Physics, Govt. College for Women, Thiruvananthapuram-695014. Kerala, India
[4] Dept. of Physics, Nesamony Memorial Christian College, Marthandam-629165, Tamil Nadu, India.
[5]Mar Baselios Institute of Technology, Anchal-691306, Kerala, India.

Corresponding Author
*__V.S. Jayakumar__, Mar Baselios Institute of Technology, Anchal-691306, Kerala, India.

E-mail: vsjkumar@gmail.com

Received on 13th January 2018
Accepted on 25th January 2018

Abstract

Antimalarial drug 5–(4–chlorophenyl)–6–ethyl–2,4–pyrimidinediamine (PYR) was investigated using FT IR and FT Raman spectra along with its molecular geometry, natural bond orbital and its molecular electrostatic potential computed using B3LYP/6–311++G (d,p) basis set. Dihedral angle between pyrimidine and phenyl rings has been extensively studied which plays an important role in the proper docking of the drug molecule in the active site of the enzyme. The strong splitting of the stretching vibrations of amino group in PYR explains the existence of intermolecular N–H···N and N–H···Cl hydrogen bonding network. MPA scheme shows that Cl_{17} atom attached to the phenyl ring is the most reactive site during electrophilic attack.

Keywords: FT-Raman, Anti-malarial, Drug activity, DFT, Pyrimidine ring

1. INTRODUCTION

Pyrimethamine (PYR) drug acts by inhibiting the dihydrofolate reductase activity of the Plasmodium falciparum enzyme dihydrofolate reductase-thymidylate synthase (PfDHFR-TS), which is involved in the reproduction of the parasite. PYR interferes with the biosynthesis of parasite by inhibiting the enzyme DHFR of plasmodia thereby blocking the biosynthesis of purine and pyrimidine which are essential for DNA synthesis and cell multiplication leading to failure of nuclear division at the time of schizont formation in the erythrocytes and liver [1]. The PYR drug shows enhanced activity in combination with Sulfadoxine. When used in combination, it produces a synergistic effect on the parasite and can be effective even in the presence of resistance to individual component [2]. The present work deals with the vibrational spectral investigations of PYR using FT-IR and NIR FT-Raman spectra along with DFT computations to analyze the structural and bonding features responsible for drug activity, nature of hydrogen bonding and charge transfer interactions.

2. EXPERIMENTAL AND COMPUTATIONAL

A Nikon Eclipse 50i microscope using an Nd: YAG laser at 1064 nm of 300 mw output as the excitation source and a liquid nitrogen-cooled Ge-diode detector with the powder sample in a capillary tube to measure the NIR-FT Raman spectrum of PYR. FT-IR spectrum of the sample was recorded using FT-IR 8400s Shimadzu spectrometer in the region 4000–400 cm^{-1} with the standard KBr pellet technique and spectral resolution was 4 cm^{-1}.

Density Functional Theoretical (DFT) computations were performed by B3LYP/ 6-311++G(d,p) basis set using GAUSSIAN'09 program package [3]. Natural bond orbital (NBO) analysis of PYR was performed using NBO 3.1 program at same level.

3. RESULTS AND DISCUSSION

3.1. Structural analysis

Optimized structural parameters of PYR (Figure 1) obtained by DFT and compared with XRD data are listed in Table 1. Slight deviations computed geometry from experimental values is probably due to the intermolecular interactions in the crystalline state. C–C bond lengths in the pyrimidine ring of C_3–C_4 (1.420 Å) is slightly increased compared with C_4–C_5 (1.397 Å) due to the presence of nitrogen. In the benzene ring, the simulated angles of C7–C8–C9 (121.39°), C8–C9–C10 (119.13°), C8–C7–C12 (117.95°), C9–C10–C11 (121.0°), C10–C11–C12 (119.11°) and C7–C12–C11 (121.42°). This deviation of the C–C–C bond angles from the normal value of 120° in the benzene ring shows the asymmetry in the benzene ring due to substitution of chlorine and pyrimidine ring.

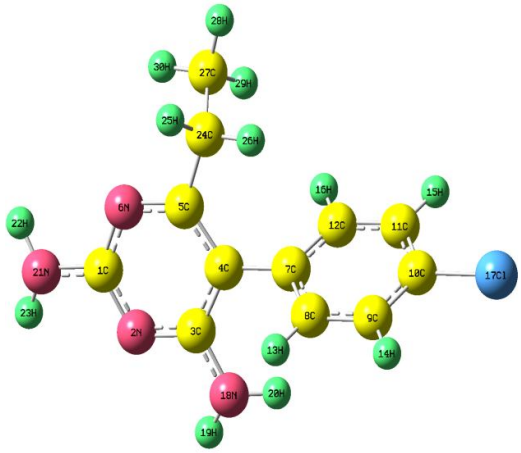

Fig. 1: Optimized molecular structure of PYR

Dihedral angles C_3–C_4–C_7–C_8 is 82.4° (78.04°) and C_5–C_4–C_7–C_{12} is 74.4° (78.92°) between 2,4–diaminopyrimidine and *p*–chlorophenyl rings confirmed pyrimethamine molecules can be described with two dihedral angles involving the pyrimidine and phenyl rings. Thus, the phenyl ring avoids coplanarity with the pyrimidine ring and attains a position approximately perpendicular to it. The same observation has been made in the modelling studies on dihydrofolate reductase-pyrimethamine complexes [4, 5] and it reveals that the relative orientation of the two rings of PYR play a key role in drug binding.

Similarly, another torsion angle C_4–C_5–C_{24}–C_{27} connecting ethyl group with pyrimidine ring is calculated to be 110.2° which represents the deviation of the ethyl group from the benzene plane while the experimental torsion angle is measured to be 97.8°. The formation of dihydrofolate reductase–pyrimethamine complexes indicate that this dihedral angle plays an important role in the proper docking of the drug molecule in the active site of the enzyme and that the change in the torsion

angle representing the orientation of the ethyl group does not affect the overall binding energy of the enzyme-drug complex [6].

Table 1: Geometrical parameters of PYR by DFT along with XRD data

Bond Length	Exp (Å)	Cal (Å)	Bond Angle	Exp. (°)	Cal. (°)	Torsion Angle	Exp. (°)	Cal. (°)
$C_1 - N_2$	1.336	1.339	$C_1–N_2–C_3$	116.47	116.36	$C_1– N_2 – C_3 – C_4$	–0.74	–0.71
$N_2 – C_3$	1.353	1.334	$N_2–C_3–C_4$	122.03	122.45	$N_2– C_3 – C_4 – C_5$	0.88	0.82
$C_3 – C_4$	1.376	1.420	$C_3–C_4–C_5$	116.17	115.56	$C_3– N_2 – C_1 – N_6$	–0.36	–0.32
$C_4 – C_5$	1.414	1.397	$N_2–C_1–N_6$	126.64	126.58	$N_2– C_3– C_4 – C_7$	179.9	117.69
$N_6 – C_1$	1.336	1.337	$C_3–C_4–C_7$	120.22	120.12	$C_3– C_4– C_7– C_8$	–81.2	–78.05
$C_5 – N_6$	1.338	1.343	$C_4–C_7–C_8$	121.08	121.23	$C_4– C_7 – C_8 – C_9$	179.6	179.60
$C_1 –N_{21}$	1.350	1.368	$C_7–C_8–C_9$	120.95	121.29	$C_7– C_8– C_9 – C_{10}$	0.17	–0.18
$C_4 – C_7$	1.492	1.492	$C_8–C_9–C_{10}$	118.80	119.13	$C_8–C_9– C_{10}– C_{11}$	–1.42	–0.14
$C_7 – C_8$	1.381	1.402	$C_9–C_{10}–C_{11}$	121.65	121.00	$C_9–C_{10}–C_{11}– C_{12}$	1.02	0.02
$C_8 – C_9$	1.389	1.392	$C_{10}–C_{11}–C_{12}$	118.91	119.11	$C_1–N_2–C_3–N_{18}$	179.6	178.24
$C_9– C_{10}$	1.366	1.391	$N_2–C_3–N_{18}$	117.12	116.16	$N_2–C_3–N_{18}–H_{19}$	178.8	164.77
$C_{10}–C_{11}$	1.359	1.391	$C_3 –N_{18}–H_{19}$	116.15	116.56	$N_2–C_3–N_{18}–H_{20}$	–13.05	11.93
$C_{11} – C_{12}$	1.385	1.393	$C_3–N_{18}–H_{20}$	122.05	119.68	$C_3–N_2–C_1–N_{21}$	179.5	177.48
$C_{12} – C_7$	1.374	1.402	$N_2–C_1 –N_{21}$	116.89	116.53	$N_2–C_1–N_{21} –H_{22}$	–172.5	–166.00
$N_{21} – H_{22}$	0.852	1.006	$C_1–N_{21} H_{22}$	117.80	117.08	$N_2–C_1–N_2 –H_{23}$	–10.01	–15.50
$N_{21} – H_{23}$	0.808	1.006	$C_1–N_{21}–H_{23}$	116.09	117.49	$C_3–C_4–C_5–C_{24}$	177.8	–179.80
$C_3 – N_{18}$	1.340	1.367	$C_5–C_{24}–H_{25}$	109.41	107.21	$C_4–C_5–C_{24} –H_{26}$	23.67	–13.16
$N_{18} – H_{19}$	0.891	1.007	$C_5–C_{24}–H_{26}$	109.41	110.35	$C_4– C_5– C_{24}–C_{27}$	–97.24	110.22
$N_{18} – C_{20}$	0.877	1.006	$C_5– C_{24}–C_{27}$	111.08	112.53	$C_5–C_{24}–C_{27}–H_{28}$	61.41	176.85
$C_{27}– H_{28}$	0.970	1.093	$C_{24}–C_{27}–H_{29}$	109.47	110.53	$C_5–C_{24}–C_{27}–H_{30}$	178.5	56.84
$C_{10}– Cl_{17}$	1.748	1.759	$C_9 –C_{10}–Cl_{17}$	119.35	119.49	$C_8–C_9–C_{10}–Cl_{17}$	178.3	179.98

3.2. Natural Bond Orbital Analysis

NBO analysis of PYR was performed and presented in Table 2 for both monomer and dimer. Lone pair interaction of $LP(1)N_{21}$ and $LP(1)N_{18}$ with anti-bonding $\pi^*(C_1–N_6)$ and $\pi^*(N_2–C_3)$ has a considerable energy difference (~55 kJ mol^{-1}), which is an evidence for charge transfer from nitrogen atom to the $\pi^*(C_1–N_6)$ and $\pi^*(N_2–C_3)$ and induces partial π character. Intermolecular charge–transfer interactions are formed by the orbital overlap between the bonding (π) and anti-bonding (π^*) orbitals. This investigation obviously clarifies the formation of two intermolecular H–bonded interactions between $LP(1)N_2$, $LP(1)N_{31}$ and $\pi^* N_{40}–H_{42}$, $\pi^* N_{18}–H_{20}$ anti-bonding orbitals respectively, illustrating the existence of strong N–H···N intermolecular hydrogen bonding in PYR supported by the XRD data.

Table 2: 2nd order perturbation theory analysis of Fock matrix in NBO basis for PYR

Donor NBO (i)	Acceptor NBO (j)	$E^{(2)}$ kcal/ mol	E(j) –E(i) a.u.	F(i,j) a.u.
$\pi C_1 – N_6$ (Monomer)	$\pi^* C_4 – C_5$	33.78	0.34	0.096
$\pi N_2 – C_3$ (Monomer)	$\pi^* C_1 – N_6$	39.14	0.31	0.104
$\pi C_4 – C_5$ (Monomer)	$\pi^* N_2 – C_3$	34.18	0.26	0.088
LP_1N_{18} (Monomer)	$\pi^* N_2 – C_3$	56.68	0.28	0.119
LP_1N_{21} (Monomer)	$\pi^* C_1 – N_6$	50.27	0.28	0.113
LP_1N_2 (Dimer)	$\pi^* N_{40} – H_{42}$	8.14	1.06	0.085
LP_1N_{31} (Dimer)	$\pi^* N_{18} – H_{20}$	7.77	1.13	0.085
LP_1N_{37} (Dimer)	$\pi^* C_{32} – N_{33}$	62.15	0.26	0.121
LP_1N_{40} (Dimer)	$\pi^* N_{31} – C_{36}$	59.58	0.26	0.119

3.3. Vibrational spectra analysis

The vibrational analysis of Pyrimethamine is performed on the basis of the characteristic vibrations of amine, Pyrimidine ring, Phenyl ring, Methyl, Methylene groups and skeletal bonds. Raman and Infrared spectra are shown in Figure 2 and 3 as well as calculated vibrational wave numbers assignments are given in Table 3.

3.3.1. Amino group vibrations

Asymmetric and symmetric amino group vibrations are usually expected in the region 3380–3350 cm^{-1} and 3310–3280 cm^{-1}, respectively [7]. Intense IR bands at 3481 and 3468 cm^{-1} correspond to the asymmetric stretching of the amino groups attached to the pyrimidine ring and symmetric stretching vibrations of the amino groups manifest as a strong IR band at 3311 cm^{-1} and at 3311 and 3324 cm^{-1} as split bands in Raman. Lowering of N–H bands provides a strong diagnostic point for detection of interaction between the drug and other molecules due to the possibility of intermolecular N–H···N and N–H···Cl hydrogen bonding hydrogen bonding.

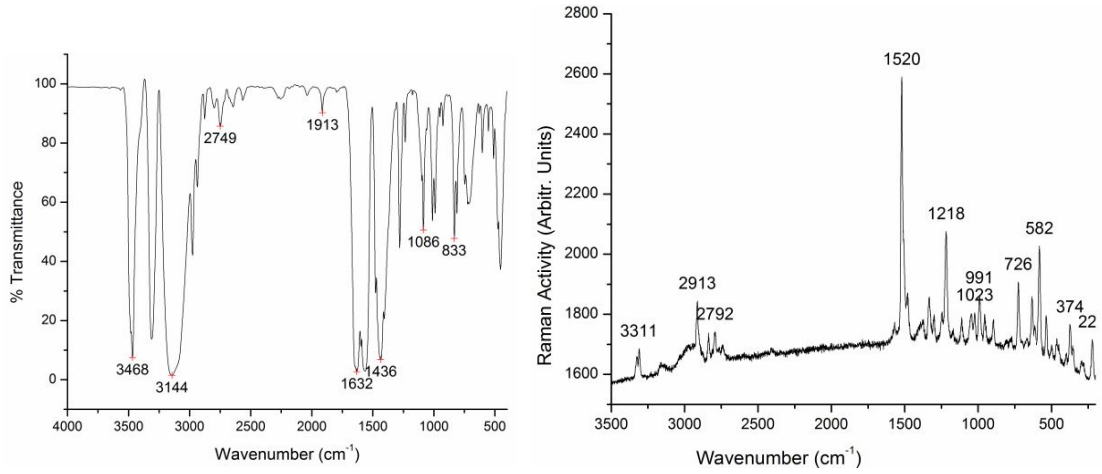

Fig. 2: FT IR and Raman spectra of PYR

3.3.2. Pyrimidine/Phenyl ring vibrations

Numbering of the vibrations of pyrimidine can generally be made by analogy with those for benzene and its derivatives proposed by Wilson. Most of the substituted pyrimidines exhibit four bands in the range 1600–1375 cm^{-1} due to aromatic ring stretches [8]. In pyrimidines, pairs of absorption bands of 8a, 8b, 19a, and 19b have been assigned as the CC and CN coupled vibrations [9]. In PYR, the vibration 8a appears as a very strong band in IR at 1560 cm^{-1} and a weak band in Raman spectrum at 1569 cm^{-1}. The most intense Raman band in PYR at 1520 cm^{-1} and at 1436 cm^{-1} in IR are correlated to very intensive C=C/C-N stretching vibrations (8b and 19b modes) of the pyrimidine ring. Phenyl ring mode *8a* manifests as very strong band in IR at 1596 cm^{-1} and the *8b* mode appears as medium Raman band at 1535 cm^{-1} being calculated at 1584 and 1552 cm^{-1}. With strong donor and acceptor substituents, the *19a* mode in *p*-disubstituted benzene can be expected in the region 1460–1530 cm^{-1} with larger intensity and *19b* appears as medium band between 1370 and 1470 cm^{-1}. The intense IR band observed at 1506 cm^{-1} corresponds to the *19a* mode while the corresponding computed wave numbers are calculated to be 1481 cm^{-1}. *19b* mode appears in Raman at 1374 cm^{-1} (calculated at 1374 cm^{-1}). Carbon-hydrogen stretching vibrations give rise to bands in the region 3100–3000 cm^{-1} in all the aromatic compounds [10]. C–H stretching vibrations in the benzene derivatives arises from two nondegenerate modes a_{1g} (3072 cm^{-1}), b_{1u} (3060 cm^{-1}) and two degenerate modes e_{2g} (3047 cm^{-1}), e_{1u} (3099 cm^{-1}), i.e. vibrations *2, 13, 7* and *20*, respectively. C–H stretching vibration *20b* is observed in IR at 3087 cm^{-1} as strong shoulder bands and the most intense IR band at 3144 cm^{-1} corresponds to ring C–H stretching mode *2*.

Table 3: Vibrational assignments for PYR

$\nu_{calculated}$	ν_{IR}	ν_{Raman}	**Assignments**
3576 3558	3481(vvssh) 3468 (vvs)		NH_2 asymmetric stretch
3459 3445	3311 (vvs)	3324 (w) 3311 (w)	NH_2 symmetric stretch
3100	3144 (vvs)	3158 (w)	2 Benzene ring vibration
3099	3087 (vssh)		20b Benzene ring vibration
3021	2975 (s)		CH_3 asymmetric stretch
3001	2937 (m)		CH_2 asymmetric stretch
2944		2913 (m)	CH_3 symmetric stretch
2933	2877 (w)		CH_2 symmetric stretch
	2800 (w) 2749 (w)	2796 (w) 2785 (w)	N-H· · ·Cl stretch / N-H· · ·N stretch
1605	1651 (vvs) 1631 (vvs)		NH_2 Scissoring
1584	1596 (vs)		8a, Benzene ring vibration
1564	1566 (vvs) 1558 (vvs)	1569 (w)	8a, PYM ring vibration
1552		1535 (vw)	8b, Benzene ring vibration
1537		1520 (vvs)	8b, PYM ring vibration
1481		1506 (ssh)	19a, Benzene ring vibration
1480		1481 (msh)	CH_3 asymmetric bending
1453	1477 (vs)		CH_2 Scissoring
1417	1436 (vvs) 1404 (vvs)		19b, PYM ring vibration/ CH_2 twisting
1379		1374 (vw)	19b, benzene ring vibration
1365		1332 (m)	CH_3 symmetric bending
1317		1298 (w)	CH_2 wagging
1282	1280 (s)		3, benzene ring vibration
1268		1246 (w)	14, benzene ring vibration
1257	1233 (m)		CH_2 Twisting
1229		1218 (s)	CH_2 Twisting
1165	1170 (vvw)	1169 (w)	9a, benzene ring vibration
1139		1113 (w)	NH_2 rocking
1092	1085 (s)		18b, benzene ring vibration
1068		1047 (w)	18a, benzene ring vibration
1046		1022 (m)	CH_3 asymmetric deformation/ NH_2 rocking
1008	1011 (s)		CH_2 Rocking

3.3.3. Methyl/Methylene vibrations

CH_3 asymmetric stretching appears at 2975 cm^{-1} in IR as strong bands and corresponding mode is computed at 3021 cm^{-1}. Symmetric CH_3 stretching mode band is observed at 2913 cm^{-1} as medium Raman band, which is calculated at 2944 cm^{-1} and the asymmetrical and symmetrical bending vibrations of methyl group occur near 1450 and 1375 cm^{-1} respectively [11]. Asymmetrical bending vibrations appear in IR at 1481 cm^{-1} as medium band while the medium Raman band at 1332 cm^{-1} is due to the symmetrical umbrella mode, which are predicted at 1480 and 1365 cm^{-1} by DFT calculations.

Methylene asymmetric and symmetric stretching bands are usually observed near 2953 and 2868 cm^{-1} respectively. Asymmetric stretching modes appear as medium IR band at 2937 cm^{-1} (calculated at 3001 cm^{-1}) while the symmetric stretching vibration is observed at 2877 cm^{-1} (calculated at 2933 cm^{-1}) in IR. Scissoring mode of the CH_2 group gives rise to a characteristic band near 1465 cm^{-1} in IR and Raman spectra which is correlated to the strong band observed at 1477 cm^{-1} in IR.

3.4. Molecular Electrostatic Potential (MESP) Analysis

Molecular electrostatic potential surface of PYR (MESP) was determined by B3LYP/6-311++G(d,p) level in order to understand the relative polarity of the molecule. The variation in electrostatic potential produced by a molecule is largely responsible for the binding of a drug to its receptor binding sites, as the binding site in general is expected to have opposite areas of electrostatic potential. The different values of the electrostatic potential at the surface are represented by different colors: red represents regions of most negative electrostatic potential, blue represents regions of most positive electrostatic potential, and green represents regions of zero potential. It is evident that the region around the hydrogen atoms of the carbon and nitrogen atoms are electron deficient (light blue color), therefore binding site for electrophiles (Figure 3). The region around the nitrogen of the pyrimidine ring represents the most electron rich region and it is the binding site for nucleophiles.

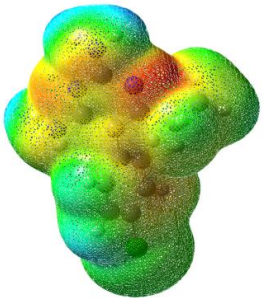

Fig. 3: Electrostatic potential at the surface

4. CONCLUSIONS

Vibrational spectra and DFT quantum chemical computations at B3LYP/6-311++G(d,p) level were performed on PYR to investigate the structural and bonding features responsible for drug activity, nature of hydrogen bonding and charge transfer interactions. Dihedral angle between the pyrimidine ring and phenyl ring indicating the coplanarity of the phenyl ring with the pyrimidine ring. NBO analysis explains the formation of two intermolecular H-bonded interactions illustrating the existence of strong N-H···N intermolecular hydrogen bonding in PYR supported by XRD data. C=C stretching vibrations are expected to be sensitive to possible drug-target interactions. From MESP map the binding sites of electrophiles and nucleophiles have been identified. MPA scheme shows that Cl_{17} atom attached to the phenyl ring, C_9 atom of the phenyl ring and few carbon atoms of the pyrimidine ring are the most reactive sites during electrophilic attack.

REFERENCES

[1] Yuvaniyama J., Chitnumsub P., Kamchonwongpaisan S., Vanichtan J., Sirawaraporn W., Taylor P., Walkinshaw M.D. and Yuthavong Y., Nature Structural Biology, 10(5), **2003,** 357–365.

[2] Anita C. Rudy and Wesley J. Poynor, Pharmaceutical Research, 7(10), **1990,** 1055–1060.

[3] Frisch M.J., et.al, Gaussian'09, Revision C.02, Gaussian Inc., Wallingford CT, **2010,**

[4] Sethuraman V. and Muthiah P.T., Acta Cryst., E58, **2002,** o817–o818.

[5] Clare E. Sansom, Carl H. Schwalbe, Peter A. Lambert, Roger J. Griffin and Malcolm and Stevens F.G. , Biochimica et Biophysica Acta, 995, **1989,** 21–27.

[6] Desiraju G.R., Angew. Chem. Int. Ed. Engl., 34, **1995,** 2311–2327.

[7] Smith B., Infrared Spectral Interpretation, a systematic Approach, CRC press, Washington, DC., **1999**.

[8] Varsanyi G., Vibrational Spectra of Benzene Derivatives, Academic Press, New York. **1969**.

[9] Dollish F.R., Fateley W.G., Bentley F.F., Characteristic Raman Frequencies of Organic Compounds, Wiley, New York., **1997**.

[10] Socrates G., Infrared Characteristic Group Frequencies, Wiley, New York. **1980**.

[11] Robert M Silverstein and Francis X Webster, Spectroscopic identification of Organic Compounds, John Wiley & Sons Inc, Sixth ed., New York., **2003**.

[12] Soni Mishra, Deepika Chaturvedi, Anubha Srivastava, Poonam Tandon, Ayala A.P. and Siesler H.W., Vibrational Spectroscopy, 53, **2010,** 112–116.